Numerical Study of Transition to Stripe Phases in High Temperature Superconductors Under a Strong Magnetic Field

Yan Chen, H. Y. Chen and C. S. Ting
Texas Center for Superconductivity and Department of Physics, University of Houston, Houston, TX 77204

The nature of spin density wave (SDW) and charge density wave (CDW) in the mixed state of high T_c superconductors (HTS) is investigated by using the self-consistent Bogoliubov-de Gennes equations and an effective model Hamiltonian with competing SDW and d-wave superconductivity interactions. We show that there exists a critical onsite Coulomb interaction U_c. For optimally doped sample, a two dimensional SDW and CDW modulations are induced for $U < U_c$ while SDW and CDW orders become antiferromagnetic (AF) and charge stripes for $U > U_c$. These stripe orders are stabilized and enhanced near the vortex cores. The wavelengths of the AF stripes and charge stripes are found respectively to be $8a$ and $4a$ with a as the lattice constant. We show that our results could be applied to understand several recent experiments on HTS.

PACS numbers: 74.20.-z, 74.25.Jb, 74.60.Ec

Intensive efforts have been focused on the searching and the understanding of spin-density wave (SDW) and other phases in the mixed state of high T_c superconductors (HTS) for the past several years. Experiments from the neutron scattering [1, 2, 3], scanning tunneling microscope(STM) [4, 5, 6], and nuclear magnetic resonance(NMR) [7] provided vital information on these topics. For example, according to the neutron scattering experiment by Lake *et al.* [2], a remarkable antiferromagnetism or SDW appears in the optimally doped $La_{2-x}Sr_xCuO_4$ when a strong magnetic field is applied. Recently, Hoffman *et al.* [6] studied the LDOS in the mixed states of optimally doped $Bi_2Sr_2CaCu_2O_{8+\delta}$ using STM measurements, and they found that associated with the SDW, anisotropic charge density wave (CDW) exists both inside and outside the vortex cores. The coexistence of d-wave superconductivity (DSC), SDW and CDW orders in terms of the stripe phases was theoretically studied in the absence of a magnetic field [8, 9, 10, 11].

Although the competition between SDW and DSC in a magnetic field was previously examined [12, 13, 14, 15], the nature of the SDW and CDW and their spatial variations have not been addressed in such detail as to compare with the experiments. In this paper, we shall adopt the method described in previous papers [16, 17] to examine the possible existence of SDW and accompanying CDW orders in the mixed state of HTS, and their nature in optimally doped samples. In order to simplify the numerical calculation, we shall assume a square vortex lattice for the mixed state and a strong magnetic field B such that $\lambda \gg b \gg \xi$ with λ as the London penetration depth, ξ the coherence length and b the vortex lattice constant. Under this condition, the applied magnetic field B can be regarded as a constant throughout the sample. Our calculation is based upon a model Hamiltonian with competing DSC and SDW orders and realistic band structure parameters. For an optimally doped sample ($x = 0.15$) under a strong magnetic field B, we find that DSC, SDW and CDW stripe phases could be in existence and they are pinned and enhanced by the vortex lattice. Numerical calculation based upon a magnetic unit cell of 48×24 lattice sites shows the wavelength of the SDW stripe to be $8a$ and the accompanying CDW stripe to be $4a$. A phenomenological model will be used to explain the anisotropic SDW and CDW observed by experiments [2, 6].

Let us begin with an effective mean field model in which interactions describing both DSC and antiferromagnetic (AF) orders in a two-dimensional square lattice are considered. The effective one band Hamiltonian can be written as:

$$H = \sum_{\mathbf{i},\mathbf{j},\sigma} -t_{\mathbf{i},\mathbf{j}} c^\dagger_{\mathbf{i}\sigma} c_{\mathbf{j}\sigma} + \sum_{\mathbf{i},\sigma} (U n_{\mathbf{i}\bar{\sigma}} - \mu) c^\dagger_{\mathbf{i}\sigma} c_{\mathbf{i}\sigma} + \sum_{\mathbf{i},\mathbf{j}} (\Delta_{\mathbf{i},\mathbf{j}} c^\dagger_{\mathbf{i}\uparrow} c^\dagger_{\mathbf{j}\downarrow} + h.c.) \, . \tag{1}$$

where $c^\dagger_{\mathbf{i}\sigma}$ is the electron creation operator and μ is the chemical potential. In the presence of magnetic field B, the hopping integral can be expressed as $t_{\mathbf{i},\mathbf{j}} = t^0_{\mathbf{i},\mathbf{j}} exp[i\frac{\pi}{\Phi_0}\int_{\mathbf{r}_\mathbf{j}}^{\mathbf{r}_\mathbf{i}} \mathbf{A}(\mathbf{r})\cdot d\mathbf{r}]$ where $t^0_{\mathbf{i},\mathbf{j}} = t$ for the nearest neighboring sites (i,j) while the next-nearest neighbor hopping $t^0_{\mathbf{i},\mathbf{j}} = t'$. The superconducting flux quanta denotes as $\Phi_0 = h/2e$. Here we choose Landau gauge $\mathbf{A} = (-By, 0, 0)$ with y as the y-component of the position vector $\mathbf{r}$. The two possible orders in cuprates are SDW and DSC which have the following definitions respectively: $\Delta^{SDW}_{\mathbf{i}} = U\langle c^\dagger_{\mathbf{i}\uparrow} c_{\mathbf{i}\uparrow} - c^\dagger_{\mathbf{i}\downarrow} c_{\mathbf{i}\downarrow}\rangle$ and $\Delta_{\mathbf{i},\mathbf{j}} = V_{DSC}\langle c_{\mathbf{i}\uparrow} c_{\mathbf{j}\downarrow} - c_{\mathbf{i}\downarrow} c_{\mathbf{j}\uparrow}\rangle/2$. In the above expressions, U and V_{DSC} are respectively the interaction strengths for SDW and DSC orders. V_{DSC}, which gives rise to the d-wave superconductivity, may come from all possibilities including AF fluctuations and electron phonon interactions. The mean-field Hamiltonian (1) can be diagonalized by solving the resulting Bogoliubov-de Gennes (BdG) equations self-consistently

$$\sum_{\mathbf{j}} \begin{pmatrix} \mathcal{H}_{\mathbf{i},\mathbf{j}} & \Delta_{\mathbf{i},\mathbf{j}} \\ \Delta^*_{\mathbf{i},\mathbf{j}} & -\mathcal{H}^*_{\mathbf{i},\mathbf{j}} \end{pmatrix} \begin{pmatrix} u^n_{\mathbf{j}} \\ v^n_{\mathbf{j}} \end{pmatrix} = E_n \begin{pmatrix} u^n_{\mathbf{i}} \\ v^n_{\mathbf{i}} \end{pmatrix} \, , \tag{2}$$

where the single particle Hamiltonian $\mathcal{H}^{\sigma}_{\mathbf{i},\mathbf{j}} = -t_{\mathbf{i},\mathbf{j}} + (Un_{\mathbf{i}\bar{\sigma}} - \mu)\delta_{\mathbf{ij}}$, and and $n_{i\uparrow} = \sum_n |u^n_{i\uparrow}|^2 f(E_n)$, $n_{i\downarrow} = \sum_n |v^n_{i\downarrow}|^2(1 - f(E_n))$, $\Delta_{ij} = \frac{V_{DSC}}{4}\sum_n (u^n_{i\uparrow}v^{n*}_{j\downarrow} + v^*_{i\downarrow}u^n_{j\uparrow}) \tanh\left(\frac{E_n}{2k_BT}\right)$, with $f(E)$ as the Fermi distribution function and the electron density $n_{\mathbf{i}} = n_{\mathbf{i}\uparrow} + n_{\mathbf{i}\downarrow}$. The DSC order parameter is defined at site i as $\Delta^D_{\mathbf{i}} = (\Delta^D_{\mathbf{i}+\mathbf{e_x},\mathbf{i}} + \Delta^D_{\mathbf{i}-\mathbf{e_x},\mathbf{i}} - \Delta^D_{\mathbf{i},\mathbf{i}+\mathbf{e_y}} - \Delta^D_{\mathbf{i},\mathbf{i}-\mathbf{e_y}})/4$ where $\Delta^D_{\mathbf{i},\mathbf{j}} = \Delta_{\mathbf{i},\mathbf{j}} exp[i\frac{\pi}{\Phi_0}\int_{\mathbf{r_i}}^{(\mathbf{r_i}+\mathbf{r_j})/2} \mathbf{A}(\mathbf{r})\cdot d\mathbf{r}]$ and $\mathbf{e}_{x,y}$ denotes the unit vector along (x, y) direction. The main procedure of self-consistent calculation is given below: For a given initial set of parameters $n_{\mathbf{i}\sigma}$ and $\Delta_{\mathbf{i},\mathbf{j}}$, the Hamiltonian is numerically diagonalized and the electron wave functions obtained are used to calculate the new parameters for the next iteration step. The calculation is repeated until the relative difference of order parameter between two consecutive iteration step is less than 10^{-4}. By varying the chemical potential, one obtains solutions corresponding to various doping concentrations.

In the following calculation, the length and energy are measured in units of the lattice constant a and the hopping integral t respectively. Here the next-nearest neighboring hopping integral is chosen to be $t' = -0.2$ to fit the band structure of HTS. It needs to be pointed out that the induction of internal magnetic field by the supercurrent around the vortex core is very small as compared with the external magnetic field, so that the uniform magnetic field distribution is a valid approximation. We follow the standard procedures [16, 17] to introduce magnetic unit cells, where each unit cell accommodates two superconducting flux quanta. Periodic boundary condition is imposed in calculation. The related parameters are chosen as the following: For optimal doping $x = 0.15$ (or the electron doping $n_f = 0.85$), the DSC coupling strength is $V_{DSC} = 1.0$, the linear dimension of the unit cell of the vortex lattice is chosen as $N_x \times N_y = 48 \times 24$ sites.

First let us choose $U = 2.2$ such that AF order is completely suppressed at zero field. Our calculation is performed at low temperature. The spatial variation of DSC order parameter Δ^D_i is plotted on a 24×24 lattice in Fig. 1(a) with the vortex core situated at the center where the DSC order parameter vanishes. By comparing it with the vortex structure of a pure DSC, the size of the vortex core here is noticeably to be enlarged. Fig. 1(b) displays the spatial variation of the induced staggered magnetization of SDW order as defined by $M^s_{\mathbf{i}} = (-1)^i\Delta^{SDW}_{\mathbf{i}}/U$. There the SDW order xists both inside and outside the vortex cores , and exhibits isotropic two-dimensional behavior with the period $8a$ along both x and y directions. Its magnitude reaches the maximum value at the vortex core center. The DSC and SDW orders coexist throuhout the whole sample. The appearance of the SDW order around the vortex cores strongly affects the spatial profile of the local electron density distribution, which can be represented by a weak CDW as shown in Fig. 1(c). The remarkable enhancement of electron density (or depletion of the hole density) is presented at the vortex core center. The variation of the electron density outside the vortex core shows weak oscillation. Different two-dimensional SDW and CDW structures have also been obtained for a different set of band parameters [18].

Next we perform the calculation at very low temperature for $U = 2.4$, the obtained results are fundamentally different from those for $U = 2.2$, and they are presented in Fig. 2. In Fig. 2(a) we plot the spatial variation of DSC order parameter. It is clear that y-axis oriented stripe like structures appear in Δ^D_i with a weakly modulation period of $4a$. The size of vortex core is further enlarged and elongated along the y axis than in Fig. 1(a). The SDW order and CDW order are displayed in Fig. 2(b) and Fig. 2(c), respectively. The SDW order behaves like almost uniform AF stripes oscillating with a wavelength of $8a$. The vortex core is always pinned at one of the ridges of AF stripes where the AF order is stronger than those at other sites. The spatial modulation of CDW order also exhibits quasi-one-dimensional charge stripes behavior with a wavelength $4a$, exactly half of that of the SDW along the x direction. The above numerical results are checked by three different set of initial parameters $n_{\mathbf{i}\sigma}$ and $\Delta_{\mathbf{i},\mathbf{j}}$ and the iteration processes have been carried out for more than 500 steps to achieve the required accuracy. The above results for finite B indicate that there exists a critical point $U_c \sim 2.25$ between $U = 2.2$ and $U = 2.4$, such that isotropic two-dimensional SDW and CDW may be induced when $U < U_c$ and they become stripe like structures when $U > U_c$. As we shall show below that the AF stripes and charge stripes obtained here could be very relevant to experiments performed on the optimally doped BSCCO. It is likely that some of the optimally doped and underdoped HTS could be close to this critical region. At $B = 0$ we found no two-dimensional SDW and CDW regardless of the value of U.

Before comparing with experiments, we would like to point out that the stripe phases oriented along x- and y-directions are degenerate in energy. In order to compare with the experiments, we shall assume that in certain domains of the sample the stripes are further pinned by some defects which makes their orientation along the y-direction more energetically favorable than those along the x-direction. Setting the energy difference between the x- oriented and y-oriented stripe phases to be $\delta E > 0$ and defining $\eta = exp(-\delta E/T)$ with T as the temperature, then the statistical probabilities for y-oriented and x-oriented stripes to appear at temperature T are respectively $1/(1 + \eta)$ and $\eta/(1 + \eta)$. The measured order parameter should be $O = [O(y) + \eta O(x)]/(1 + \eta)$ with $O(x)$ $[O(y)]$ representing the order parameter for one of the x- (y-) oriented DSC, AF and charge stripes. The combined results are shown in Fig. 3 for $\eta = 0.5$. The spatial variation of the combined superconductivity order parameter is presented in Fig. 3(a). Here the SDW (see Fig.3(b)) and CDW (see Fig.3(c)) have anisotropic two dimensional structures and respectively with periodici-

ties $8a$ and $4a$, in good agreements with the observations of Lake *et al.* [2] and Hoffman *et al.* [6]. Our results also predict that as T approaches zero or $\eta = 0$, AF and charge stripes should show up, and at higher T or η close to 1, the observed SDW and CDW should become more isotropic. It is useful to point out that the way to explain these experiments may not be unique. As suggested by Howald *et al.* [19], if x-oriented and y-oriented stripes are pinned in two nearest neighboring domains, the proximity effect may cause these two different oriented stripes permeating each other and make their spatial distribution to look more two- dimensional like. So far we are not able to numerically simulate this situation.

The features exhibited in Fig. 2 and Fig. 3 are very robust when $U > U_c$. We believe that the optimally doped BSCCO sample should have a $U > U_c$. While the STM experiments [6] were performed at $B \simeq 7$ Tesla, our numerical results based upon the 48×24-sites calculation corresponding to a magnetic field $B \simeq 27$ Tesla. For a realistic comparison with experiments, one needs to do a 92×46 -sites calculation, that is beyond our current computing capability. In a weaker field $B \simeq 7$ Tesla, we expect that the SDW and CDW structures with periods $8a$ and $4a$ should still exist in the neighborhood of a vortex core. Away form the vortex core, the situation should be corresponding to $B = 0$ case.

We have also done a numerical study for $B = 0$ with $U = 2.4$ and $x = 0.15$, and our calculation indicates that both the stripe phase and the uniform DSC phase (no SDW and CDW) could show up depending on the initial input parameters. Since $U = 2.4$ is quite close to U_c, the free energy difference between the stripe phase and the uniform DSC phase is estimated to be very small, which suggests that the experimental observed phase at finite temperature should come from a superposition of these two configurations. This consideration would dramatically reduce the amplitudes of the SDW and CDW stripes measured by experiments. But when a magnetic field B is applied, the stripe phase is the only solution regardless of the initial parameters. This result implies that the SDW and CDW orders are stabilized and enhanced near the vortex core within a distance of several coherence lengths. Away from the vortex core they are somewhat suppressed. Of course, the stripe phase order at $B = 0$ could be stabilized by the presence of defects and it can also be strengthened by a larger U. The enhancement of AF order near the vortex core in a strong magnetic field is consistent with neutron scattering experiments [1, 3]. Here The manifestation of stripe phases in optimally doped sample seems to be against common consensus. But our stripes are small one-dimensional SDW and CDW modulations in a d-wave superconducting background. This is different from what was proposed originally by Emery and Kivelson [8] for underdoped sample where the AF phases are insulators (no hole regions) and charge stripes are conductors (rich hole regions). There is no physical reason to forbid our stripe like modulations appearing in optimum doped HTS. The observation of charge stripes in very recent STM experiments [19] at $B = 0$ seems to suggest that stripe phases may indeed be present in optimally doped BSCCO samples.

For the purpose to have a better understanding of the doping effect, the underdoped case ($x = 0.10$) is examined. We found that the spatial distribution of SDW and CDW still exhibits the stripe-like behavior as shown in Fig. 2, and the periods of SDW and CDW now change respectively to $12a$ and $6a$. We expect that the periods could even become $16a$ and $8a$, when the doping level is further reduced. These results are in qualitative agreement with the observations of Lake *et al.* [3] where a magnetic field induced AF order was observed in underdoped sample. A detailed study of the doping dependence will be reported elsewhere.

Finally, we would like to point out that Zhu *et al.* [20]did almost the same calculation using slightly larger $U = 2.5$ and $x = 0.16$, their results yield isotropic two-dimensional SDW and CDW, which are very different from the AF and charge stripes obtained by us. We have carefully checked their calculations and found that if they increased the number of iteration steps sufficiently to achieve higher accuracy, their two-dimensional SDW and CDW checkerboard patterns would have evolved into our stripe like structures as shown in Fig.2.

In summary, the stabilization and the enhancement of AF and charge stripes in a d-wave superconductor near a vortex core are numerically studied by a mean field Hamiltonian. We found the wavelength of the AF stripes to be $8a$ and that of charge stripes to be $4a$. Assuming that the degeneracy of the x-oriented and y-oriented stripe phases is broken by some defects, we show that the observed spatial variations of SDW and CDW are anisotropic and two-dimensional, with wavelengths in good agreement with experiments. We also would like to emphasize that our self-consistent mean field BdG equation calculation tends to overestimate the stability of the static AF order. In order to partially overcome this deficiency, we choose the onsite Coulomb interaction $U = 2.4$ to be somewhat smaller than that for the standard Hubbard model. The effect due to the dynamic SDW has not been included in this study. Any attempt to do the present type of calculation by including this effect is quite difficult and has to be confined to much smaller magnetic unit cell. This would make the comparison with experiments difficult. As to whether a static AF order could exist in optimally doped sample is still a subject for debate. The coexistence of charge stripes with DSC at $B = 0$ observed by very recent STM experiments [19] at optimal doping may indicate that static AF stripes are also in presence. For a pure DSC, the local density of states (LDOS) at the vortex center is well known to have a broad peak around $E = 0$ [16]. However, the vanishing LDOS at $E = 0$ near the vortex core observed by STM experiments [4, 5] for YBCO and BSCCO has been understood in terms of the presence of SDW in a d-wave superconductor [18], an indirect evidence of the existence

of the static AF order in optimally doped HTS samples. In view of all these and the favorable comparison with experiments, The qualitative feature of our results should still remain even in a more refined theory.

We wish to thank Prof. S. H. Pan and Dr. J. X. Zhu for useful discussion. This work was supported by a grant from the Robert A. Welch Foundation and by the Texas Center for Superconductivity at the University of Houston through the State of Texas.

[1] S. Katano *et al.*, Phys. Rev. B **62**, R14677 (2000).
[2] B. Lake *et al.*, Science **291**, 1759 (2001); B. Lake *et al.*, cond-mat/0104026.
[3] B. Lake *et al.*, Nature **415**, 299 (2002).
[4] I. Maggio-Aprile *et al.*, Phys. Rev. Lett. **75**, 2754 (1995).
[5] S. H. Pan *et al.*, Phys. Rev. Lett. **85**, 1536 (2000).
[6] J. E. Hoffman *et al.*, Science **295**, 466 (2002).
[7] V. F. Mitrovic *et al.*, Nature **413**, 501 (2001).
[8] V. J. Emery and S. A. Kivelson, Physica C **209**, 597 (1993); V. J. Emery, S. A. Kivelson, and J. M. Tranquada, Proc. Natl. Acad. Sci. USA **96**, 8814 (1999);
[9] L. Balents, M. P. A. Fisher, and C. Nayak, Int. J. Mod. Phys. B **12**, 1033 (1998).
[10] M. Vojta, and S. Sachdev, Phys. Rev. Lett. **83**, 3916 (1999).
[11] I. Martin, *et al.*, Int. J. Mod. Phys. B **14**, 3567 (2000).
[12] D. P. Arovas *et al.*, Phys. Rev. Lett. **79**, 2871 (1997); J.-P. Hu, and S. C. Zhang, cond-mat/0108273.
[13] M. Ichioka, M. Takigawa, and K. Machida, J. Phys. Soc. Jpn. **70**, 33 (2001).
[14] E. Demler, S. Sachdev, and Y. Zhang, Phys. Rev. Lett. **87**, 067202 (2001); Y. Zhang, E. Demler, and S. Sachdev, cond-mat/0112343.
[15] D. H. Lee, Phys. Rev. Lett. **88**, 227003 (2002).
[16] Y. Wang and A. H. MacDonald, Phys. Rev. B **52**, R3876 (1995).
[17] Jian-Xin Zhu, and C. S. Ting, Phys. Rev. Lett. **87**, 147002 (2001).
[18] Yan Chen, and C. S. Ting, Phys. Rev. B **65**, R180513 (2002).
[19] C. Howald *et al.*, cond-mat/0201546.
[20] Jian-Xin Zhu, I. Martin, and A. V. Bishop, cond-mat/0201519.

FIG. 1: Spatial variations of the DSC order parameter $\Delta_{\mathbf{i}}^D$ (a), staggered magnetization $M_{\mathbf{i}}^s$ (b), and electron density $n_{\mathbf{i}}$ (c) in a 24×24 lattice. The size of a magnetic unit cell is 48×24, corresponding to a magnetic field $H = \Phi_0/(24 \times 24)$. The strength of the on-site repulsion $U = 2.2$ and the averaged electron density $\bar{n} = 0.85$.

FIG. 2: Spatial variations of the order parameters $\Delta_{\mathbf{i}}^D$ (a), $M_{\mathbf{i}}^s$ (b), and $n_{\mathbf{i}}$ (c). The strength of the on-site repulsion $U = 2.4$. The other parameter values are the same as Fig. 1.

FIG. 3: Spatial profiles of the combined x- and y- oriented stripes with the order parameters $\Delta_{\mathbf{i}}^D$ (a), $M_{\mathbf{i}}$ (b), and $n_{\mathbf{i}}$ (c). Only the 20×20 lattice with the vortex core at the center is plotted in (c). The mixing factor is chosen as $\eta = 0.5$. The other parameter values are the same as Fig. 2.

Fig. 1(a) Chen et al.

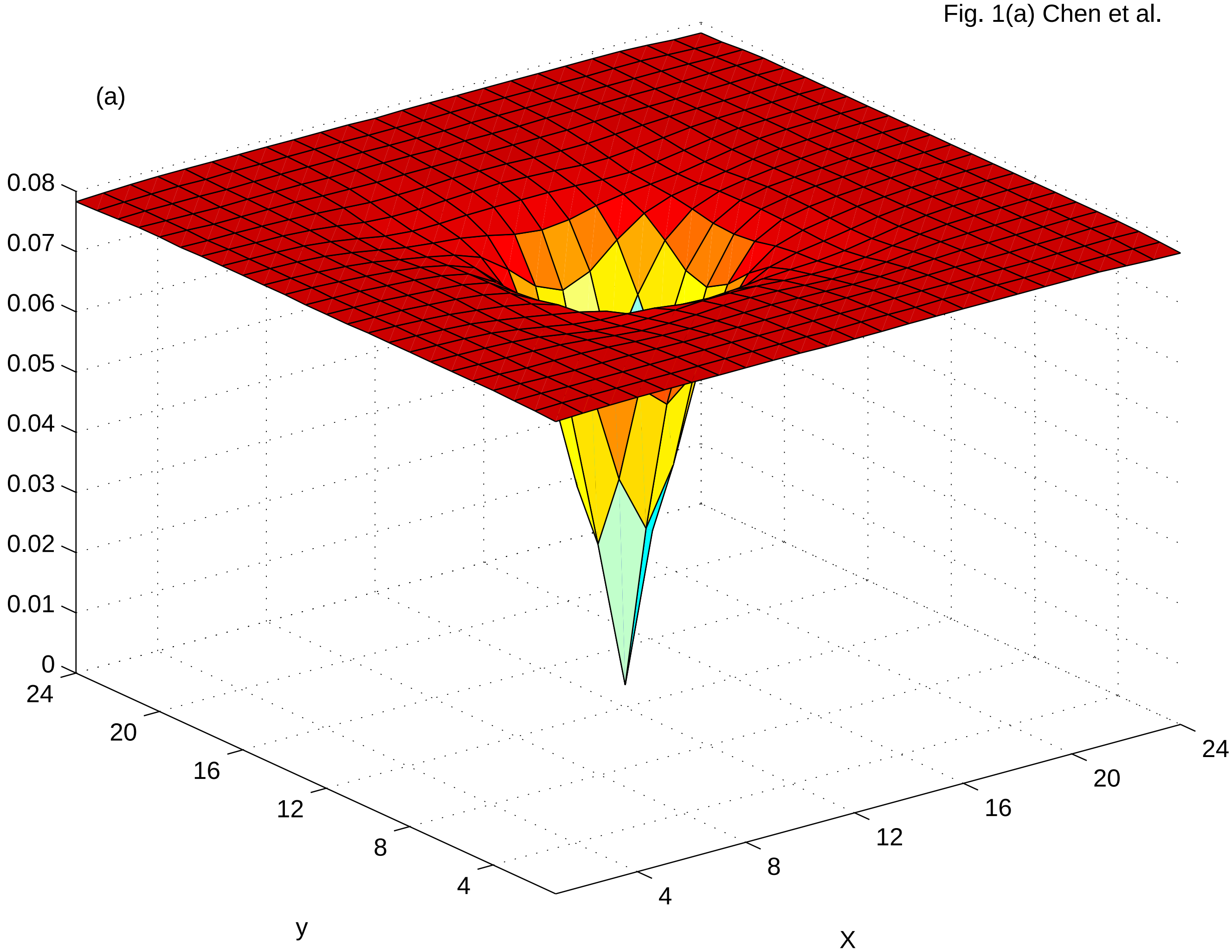

Fig. 1(b) Chen et al.

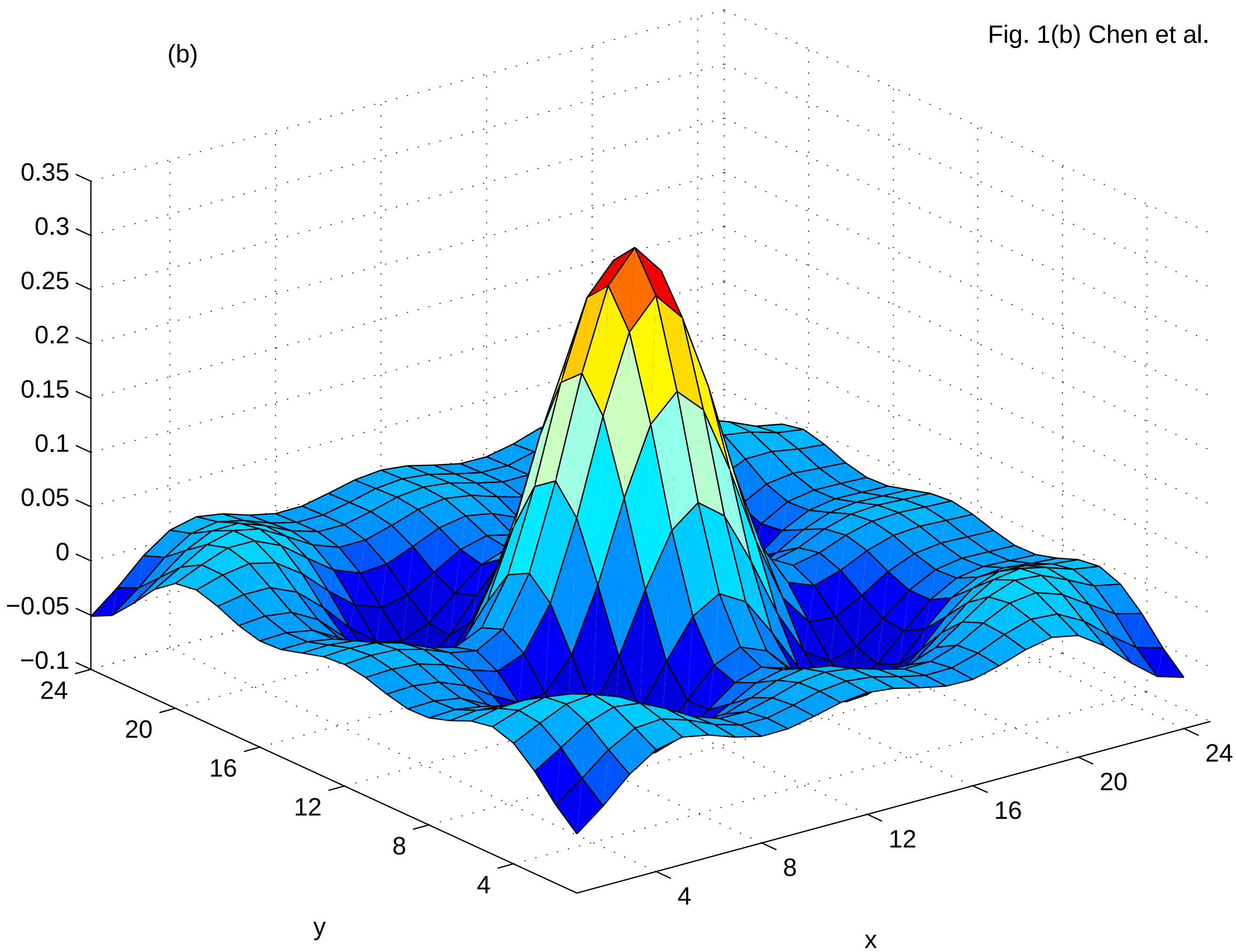

Fig. 1(c) Chen et al.

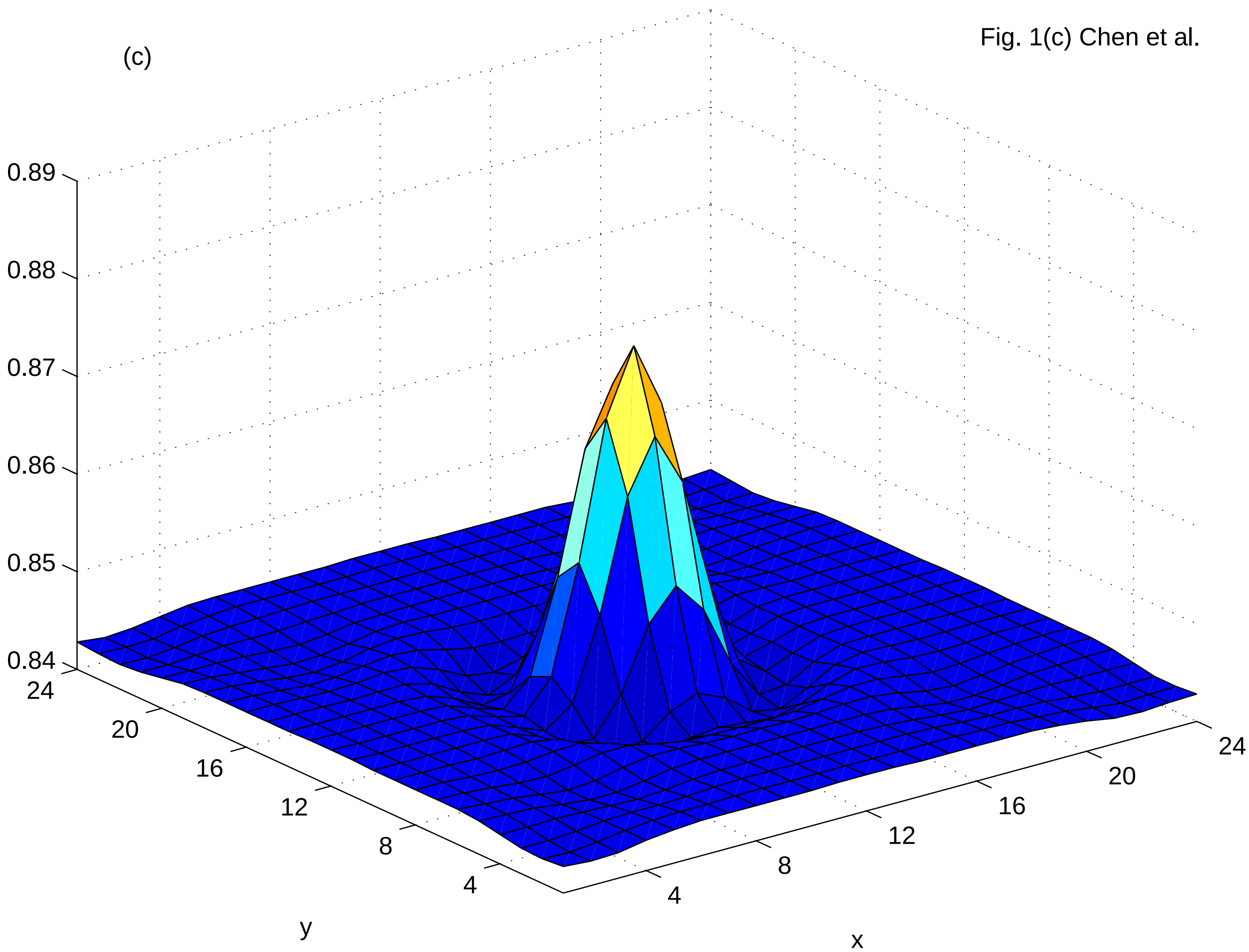

Fig. 2(a) Chen et al.

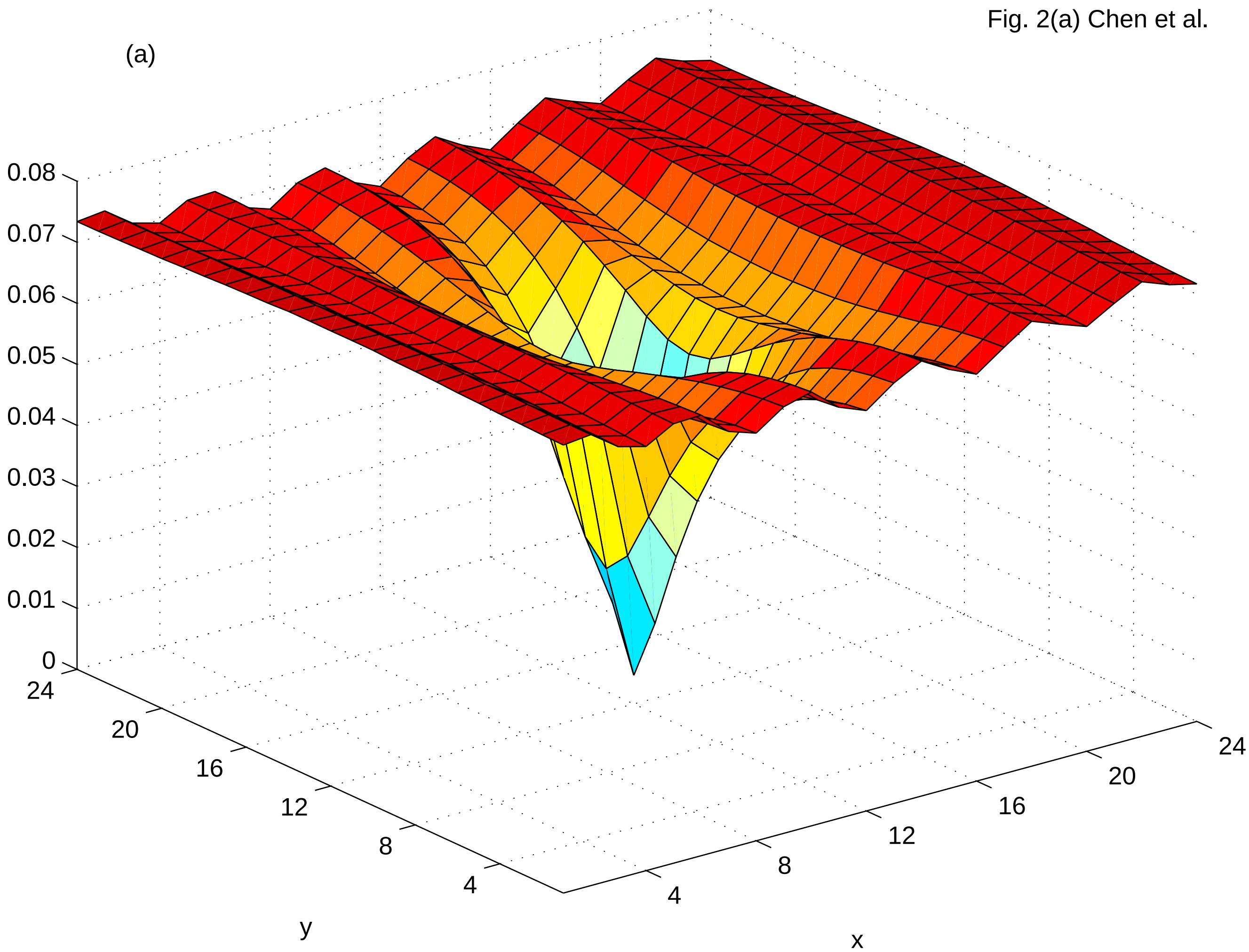

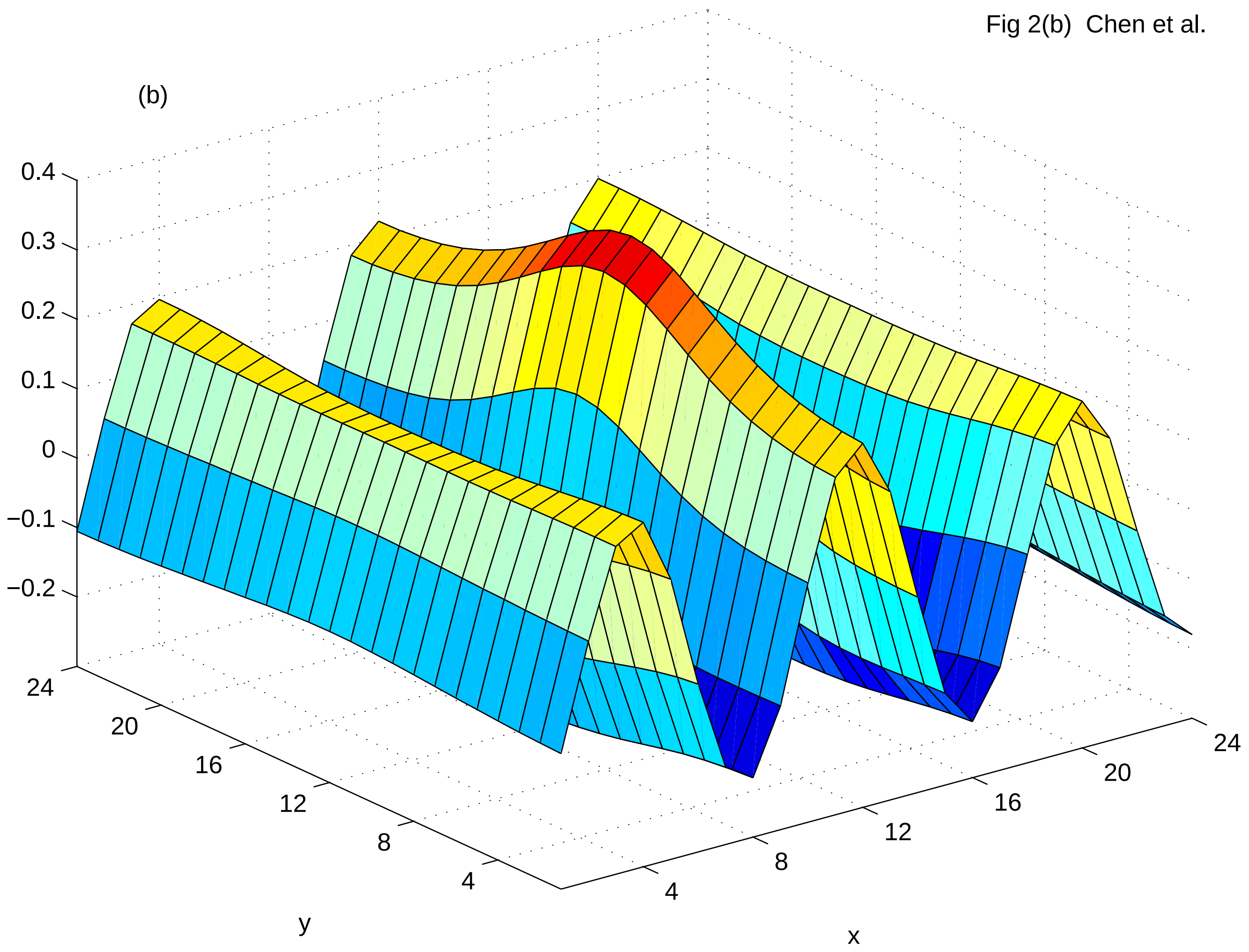
Fig 2(b) Chen et al.
(b)
0.4
0.3
0.2
0.1
0
−0.1
−0.2
24
20
16
12
8
4
y
4
8
12
16
20
24
x

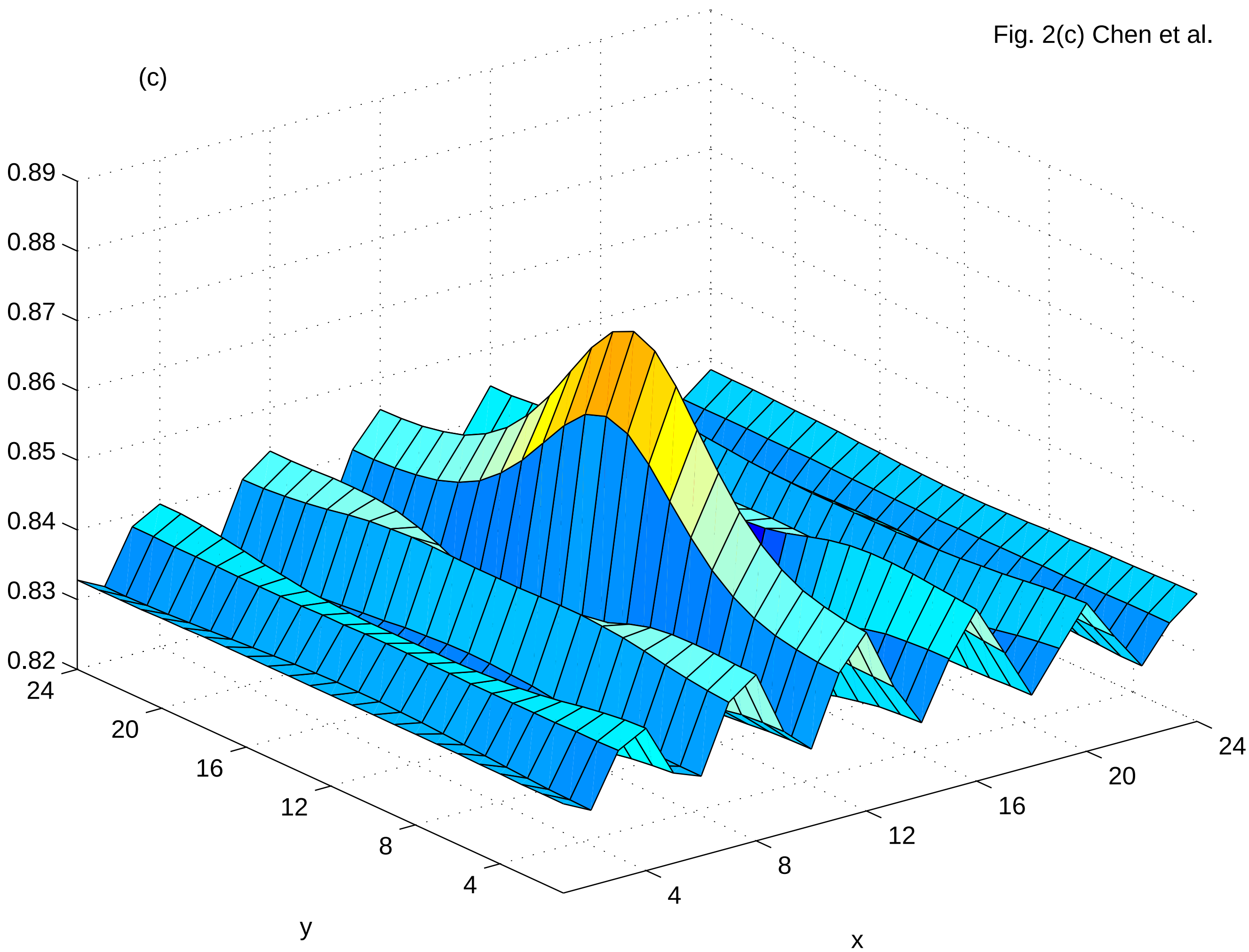

Fig. 2(c) Chen et al.

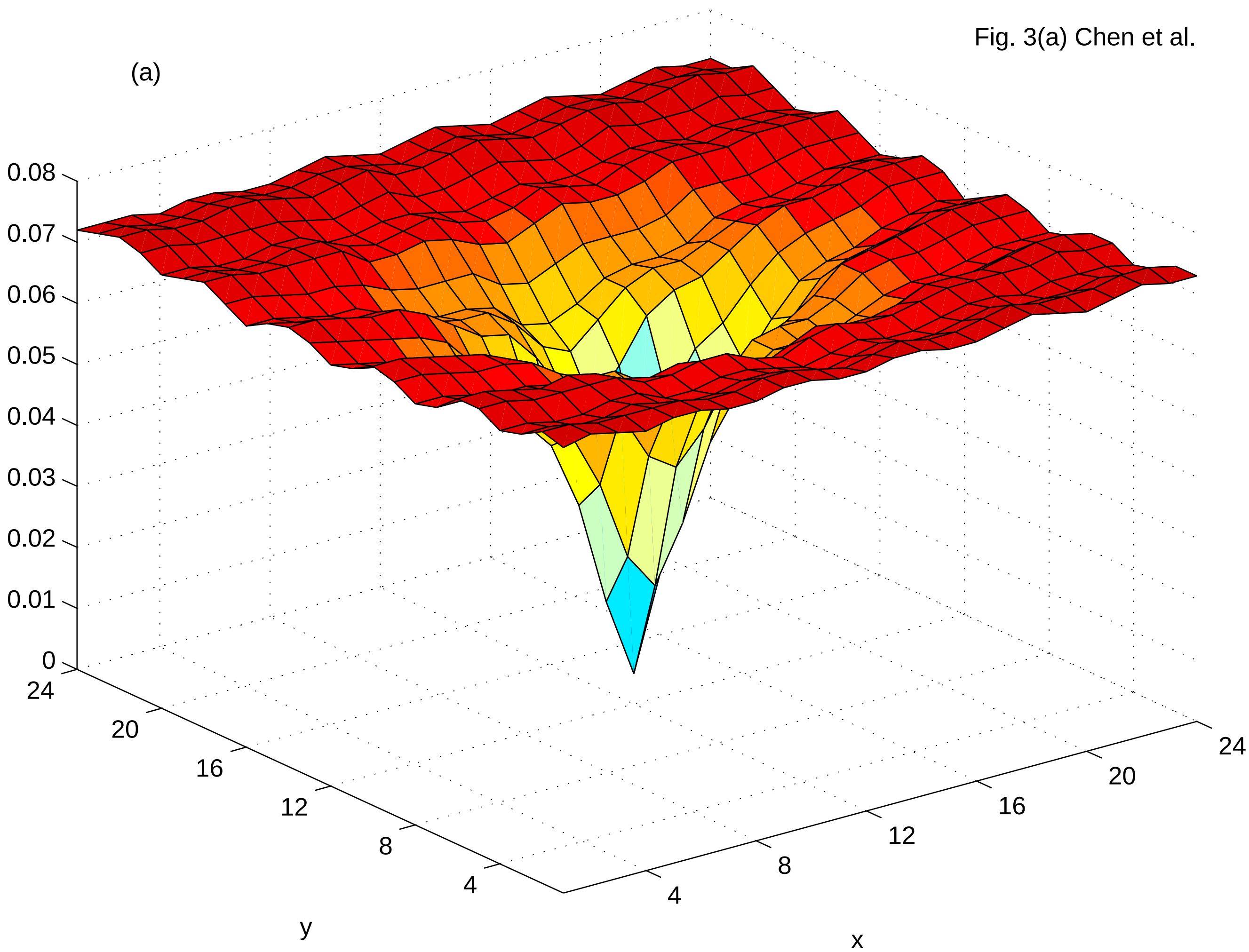
(a)
Fig. 3(a) Chen et al.
0.08
0.07
0.06
0.05
0.04
0.03
0.02
0.01
0
24
20
16
12
8
4
y
4
8
12
16
20
24
x

Fig. 3(b) Chen et al.

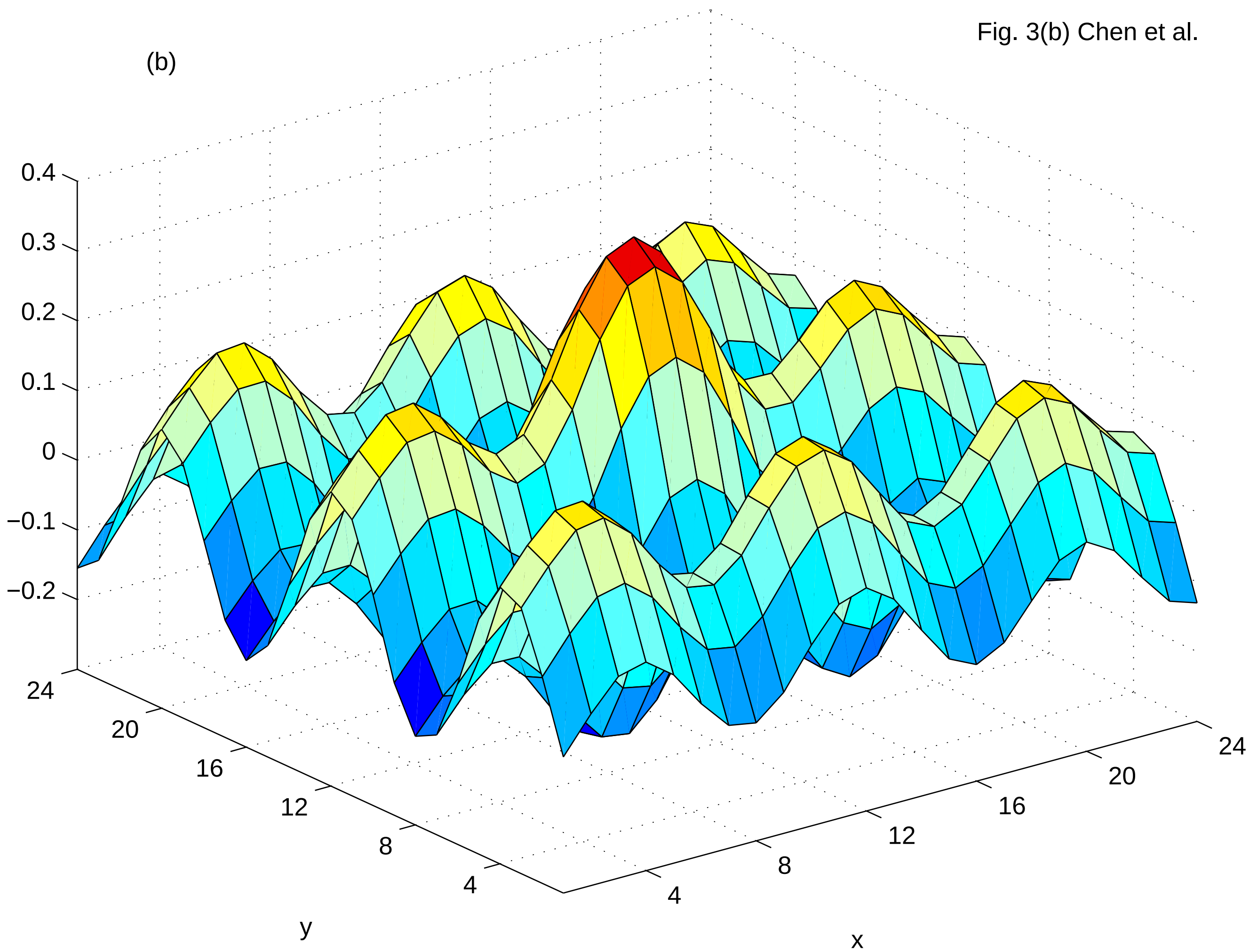

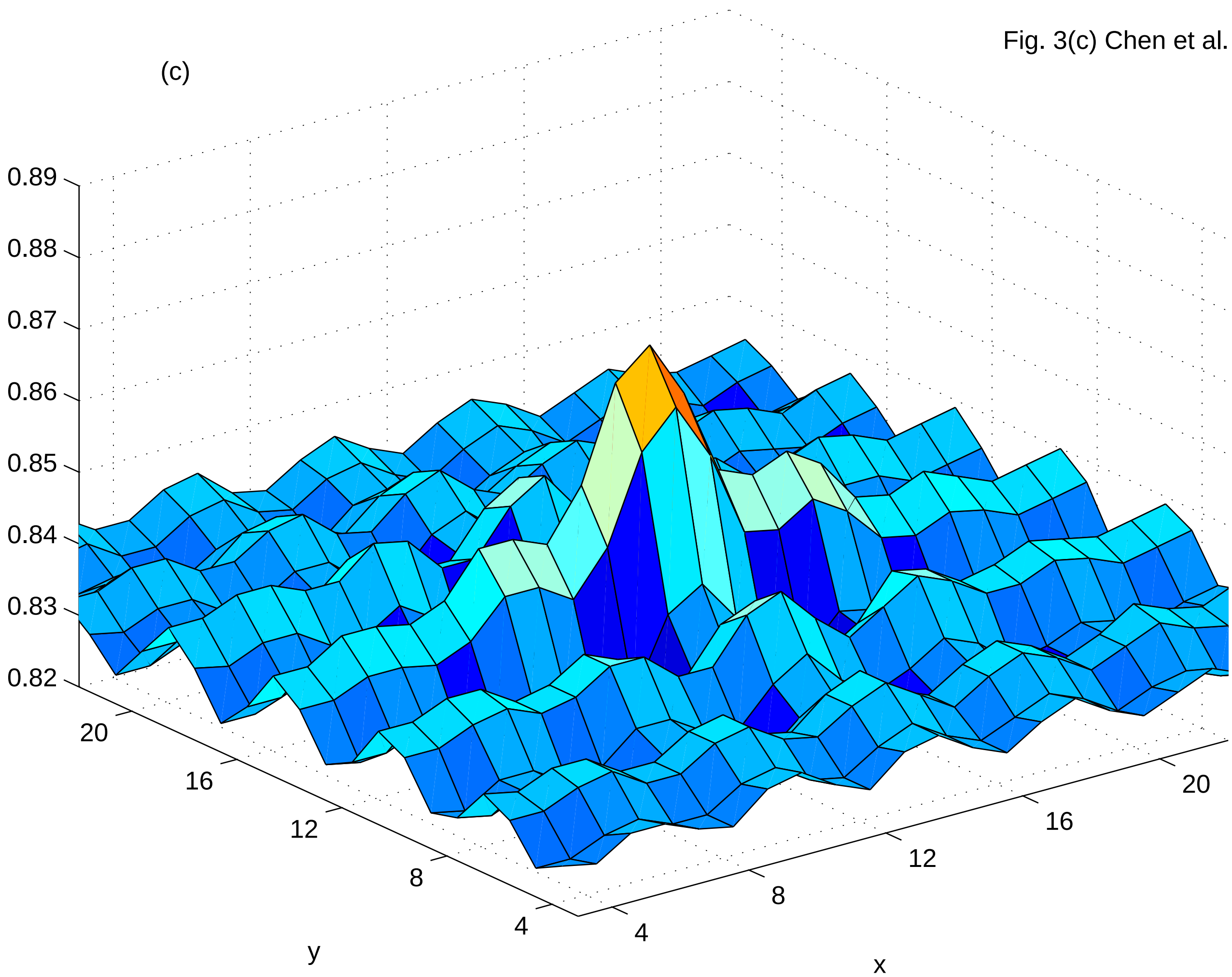

Fig. 3(c) Chen et al.
(c)
0.89
0.88
0.87
0.86
0.85
0.84
0.83
0.82
20
16
12
8
4
y
4
8
12
16
20
x